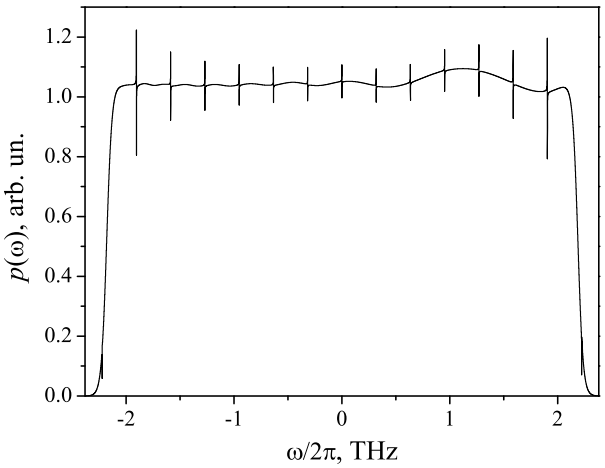

Fig. 5. Numerical spectrum for ε_l =-0.0025 and Ω_l =1 GHz and another parameters described in Table 1.

cluded a 6.3-mm thick YAG plate, 5 highly-reflective mirrors and an output coupler. The overall round-trip dispersion is computed using the known material and mirror coating data and is shown in Fig. 6, *a*. Since the zero-dispersion wavelength at 2450 nm coincided with the gain maximum of the material, it was possible to operate the laser in both, soliton and chirped-pulse regimes [25]. In the first case, the laser spectrum was centered near 2500 nm, and was in the region of the anomalous dispersion. The pulses of ≈100 fs duration did not carry any significant chirp, and the spectrum contained all the typical features of intracavity absorption as described in Ref. [13]. This regime was rather unstable because of the fast increase of water vapor absorption beyond 2500 nm. In the second regime, the laser operated with its spectrum shifted towards 2300 nm, emitting strongly chirped pulses of about 1 ps duration (Fig. 6, *b*). This regime was stable with the main part of the spectrum well in the normal dispersion region. At 91 MHz repetition rate the average output power was 170 mW through the 1.8% output coupler, corresponding to 1.9 nJ output pulse energy or 100 nJ intracavity pulse energy.

Figure 6, *a* clearly demonstrates typical dispersion-like features superimposed on the smooth pulse spectrum, as predicted by the solution Eq. (15). For quantitative analysis, it is convenient to single out the modulation part of the solution [Eq. (15)] and revert the normalizations:

$$\frac{p'(\omega)}{p(\omega)} = 1 + \frac{1}{\beta\Delta^2}\sum_{l=1}^{N}\frac{2\varepsilon_l}{1-\omega_l^2/\Delta^2}\frac{(\omega-\omega_l)/\Omega_l}{1+(\omega-\omega_l)^2/\Omega_l^2}, \tag{18}$$

where now the observables β and Δ can be directly accessed as the group delay dispersion and spectrum half-width in circular frequency units, respectively. Recalling that $q=\beta\Delta^2$ is the chirped soliton wavenumber, we see that this result has the same form as Eq. (17) in Ref. [13]. The principle difference lies with the frequency dependence of the modulation depth. While the chirped soliton exhibits resonance enhancement towards spectrum edges as $(1-\omega_l^2/\Delta^2)^{-1}$, the modulation depth for conventional soliton would decrease as $(1+\omega_l^2T_0^2)^{-1}$ (Eq. (14) in Ref. [13]).

Applying numerical values to the spectrum in Fig. 6, *a* can not be performed as straitforwardly as in [13], because the pulse spectrum strongly deviates from the symmetric profile with cut wings, required by the expression (15) due to the large third-order dispersion (51000 fs^3 at 2400 nm). Detailed description of the third-order dispersion influence on dissipative soliton is beyond the scope of this work, but for our purposes it is sufficient to estimate the 2Δ parameter,

#149532 - $15.00 USD Received 20 Jun 2011; revised 28 Jul 2011; accepted 5 Aug 2011; published 22 Aug 2011

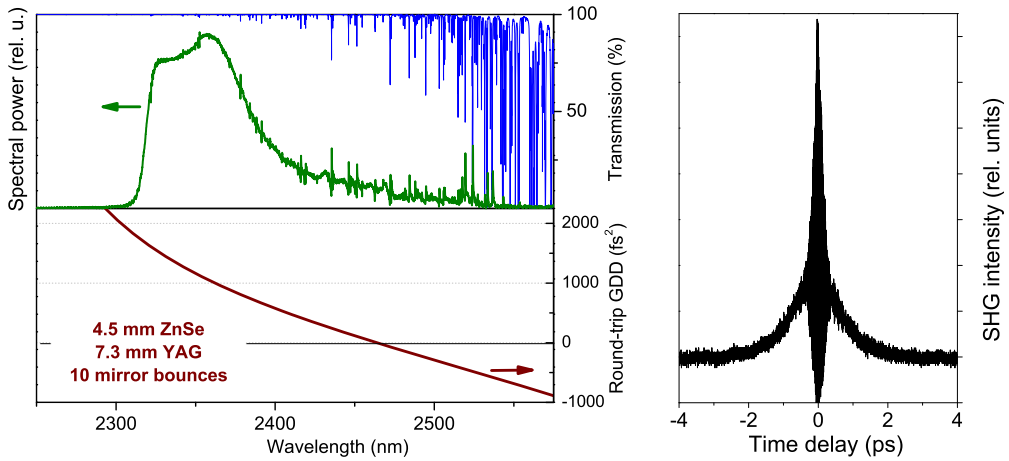

Fig. 6. Kerr-lens mode-locked Cr:ZnSe laser in normal dispersion regime. (a) Round-trip dispersion and output spectrum (note that the GDD curve presented here corrects the data of Ref. [25] by accounting for the mirrors' dispersion.) The round-trip transmission of the atmosphere (HITRAN) is shown in blue. (b) The autocorrelation trace of the chirped pulse.

for which we take the full width at half maximum $2\Delta = 70 \pm 5$ nm. Taking $\beta = 1100 \pm 100$ fs^2 in the central part of the spectrum we obtain $\beta\Delta^2 = 0.155 \pm 0.025$, i.e. (6.5 ± 1)-fold enhancement of the intracavity modulation with respect to the absorption peak. Fig. 7 shows the expanded central part of the measured spectrum along with the absorption lines, calculated from HITRAN database, assuming the measured conditions of 30±2% relative humidity and 23.5 ± 0.5 °C at the time of experiment. The observed 6-fold enhancement of the modulation amplitude is in a very good agreement with the estimation, well within the uncertainty in β and 2Δ parameters.

Finally, it is instructive to express the modulation amplitude $|\varepsilon_l/q|$ at $\omega_l = \omega \pm \Omega_l$ through the observable parameters, such as spectrum FWHM $\Delta\nu$ and round-trip GDD β, peak absorption $\chi_l L = 2\varepsilon_l$ over the round-trip intracavity absorber path length L, equal to the double resonator length in our case:

$$\left|\frac{\varepsilon_l}{q}\right| = \frac{\chi_l L}{2}\frac{1}{\beta\Delta^2} = \chi_l L \frac{0.0507}{\beta(\Delta\nu)^2}. \tag{19}$$

The numerical coefficient $1/2\pi^2 \approx 0.05066$ in the numerator differs only by a factor of 1.6 from the corresponding coefficient $\operatorname{arccosh}(3)^2/\pi^4 \approx 0.0319$ obtained for a chirp-free conventional soliton [13]. The good agreement with the experiment suggests also that this relation is quite tolerant to the presence of higher-order dispersion, as already observed in [13], and to the deviation of the the spectrum from analytical expression.

The fact that the analytical form and numerical expressions for the intracavity signal in so different regimes of operation coincide within a small correction factor allows making a more general statement. In particular, we suggest that the spectral modulation caused by a narrow-band inracavity absorber in *any* passively modelocked laser has a form of the associated index of refraction, with the modulation amplitude at the spectrum center depending only on the absorber coefficient, pulse spectrum width, and GDD parameter. It is given by the expression (19) with a correction factor, close to unity. At the same time, the behavior of modulation amplitude at the spectrum wings does depend upon the spectrum shape and chirp.

#149532 - $15.00 USD Received 20 Jun 2011; revised 28 Jul 2011; accepted 5 Aug 2011; published 22 Aug 2011

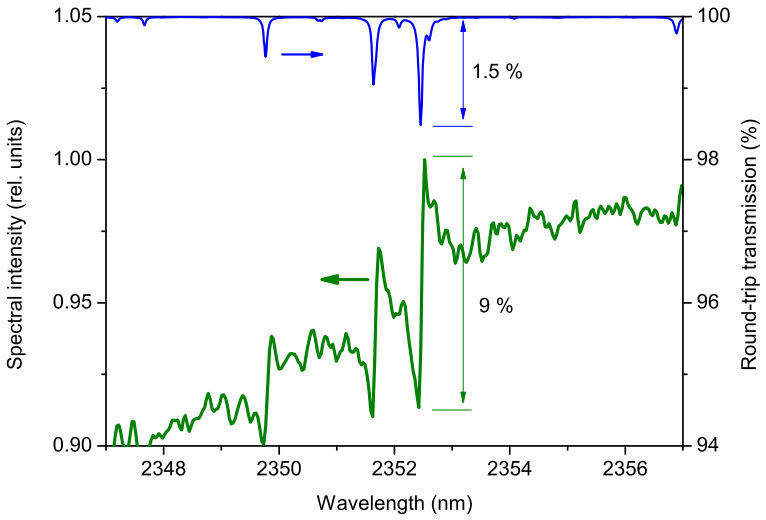

Fig. 7. Modulation signal due to the atmospheric water-vapour lines in the Cr:ZnSe laser, central part expanded. The percentage marks show the peak line absorption ($2\varepsilon_l L$) and signal amplitude ($2\varepsilon_l/\beta\Delta^2$) between the peaks at $\omega = \Omega_l \pm \omega_l$.

Formula (19) also provides means to estimate the energy content of the extended pulse tail in the time domain, discussed in Section 2. Since the time constant of this tail is much longer than the pulse duration, its overlap with the main pulse is negligible. We can therefore assume that the energy content of the tail equals the total energy of the perturbation signal $f(t)$ and calculate the energy fraction within the tail as

$$\frac{E_{tail}}{E_{pulse}} \approx \frac{1}{\beta\Delta^2}\sum_{l=1}^{N}\frac{2\varepsilon_l\cdot\pi}{1-\omega_l^2/\Delta^2} = \frac{0.05}{\beta(\Delta\nu)^2}\sum_{l=1}^{N}\frac{S_l}{1-\omega_l^2/\Delta^2}, \tag{20}$$

where S_l is the integrated absorption of the lth line over the cavity round-trip. Neglecting the enhancement factor $1/(1-\omega_l^2/\Delta^2)$ we finally obtain a practical estimation formula, valid for any passively modelocked laser:

$$\frac{E_{tail}}{E_{pulse}} = (0.04\pm 0.01)\cdot\frac{S}{|\beta|(\Delta\nu)^2}, \tag{21}$$

where S is the total integrated intracavity absorption over the spectrum width $\Delta\nu$.

5. Conclusion

Summarizing, we present an analytical theory of dissipative soliton absorption spectroscopy. We demonstrate that a dissipative soliton formed in a net-normal-dispersion oscillator with a narrowband intracavity absorber acquires spectral features that follow the index of refraction of the absorber. Similarly to the case of soliton absorption spectroscopy in an anomalous dispersion regime [13], we observe over tenfold enhancement of the spectral signal induced by an absorption line on the pulse spectrum in comparison to the conventional absorption signal. The signal enhancement inversely scales with the dispersion and the square of the spectrum width and can be controlled experimentally. In contrast to the soliton absorption spectroscopy in an anomalous dispersion regime, we anticipate resonant enhancement of the modulation signal near the pulse spectrum edges that results in additional signal gain. In the time domain, the

#149532 - $15.00 USD Received 20 Jun 2011; revised 28 Jul 2011; accepted 5 Aug 2011; published 22 Aug 2011

pulse acquires a tail with characteristic time constant defined by the inverse linewidth of the absorber.

The validity of the developed theory is confirmed by results of the numerical simulations and by experimental evidence in a Cr:ZnSe laser oscillator operating in the chirped-pulse regime. The quantitative result and qualitative dependence of the signal on laser parameters are very close to those for the conventional soliton [13] and probably hold for any passively mode-locked laser. The results are particularly interesting for the ultrabroadband femtosecond solid-state and fiber laser sources operating at wavelengths near and above 1.5 μm. They can be used to calculate the influence of the atmospheric absorption on oscillator parameters and for designing sensitive quantitative intracavity measurements.

Acknowledgments

VLK acknowledges the support of the Austrian Fonds zur Föerderung der wissenschaftlichen Forschung (FWF project P20293), ITS acknowledges the support of the Norwegian Research Council (project 191614/V30).

#149532 - $15.00 USD Received 20 Jun 2011; revised 28 Jul 2011; accepted 5 Aug 2011; published 22 Aug 2011